Jurnal Serambi Engineering JSE
Volume XI, No.4, Oktober 2026 Hal 21893 - 21902
p-ISSN : 2528-3561
e-ISSN : 2541-1934

Effect of Silica Content on the Physical, Mechanical, and Biodegradation Properties of Whey Protein Isolate/Carboxymethyl Cellulose Biocomposite Films for Food Packaging

Mukhlishien*, Azwar

Chemical Engineering Department, Universitas Syiah Kuala, Banda Aceh
***Corresponding author**: mukhlishien@usk.ac.id

Received: October 24, 2026 Approved: November 12, 2026

Abstract
Whey protein isolate (WPI)/carboxymethyl cellulose (CMC) films are promising biodegradable food packaging materials, but they suffer from low strength and high water sensitivity. This study examined the effect of silica (0–0.45 g) on WPI/CMC films containing 0.75 or 1.0 g CMC. Thickness, swelling, tensile strength, elongation at break, soil-burial biodegradation, SEM, and FTIR were evaluated. Silica increased thickness from 0.126–0.145 mm to 0.350–0.371 mm and reduced swelling from 83.23% to 63.33% (0.75 g CMC) and from 79.23% to 60.86% (1.0 g CMC). Tensile strength peaked at 0.35 g silica, reaching 27.07 MPa (0.75 g CMC), 13.4 times the control, then declined at 0.45 g, consistent with particle agglomeration seen by SEM. The highest elongation at break (58.52%) occurred with 1.0 g CMC and 0.05 g silica. Biodegradation decreased with silica loading, from about 83% to 60% (0.75 g CMC) and from about 75% to 59% (1.0 g CMC), with nearly all films meeting the SNI 7188.7:2016 threshold of 60%. FTIR revealed no new bands except Si–O–Si, indicating physical interactions without chemical modification of the polymers. Silica-filled WPI/CMC films therefore show potential as water-resistant, biodegradable packaging, with 0.05–0.35 g silica as the useful range.
Keywords: *whey protein isolate; carboxymethyl cellulose; silica; biocomposite film; biodegradability; food packaging*

Abstrak
Film whey protein isolate (WPI)/carboxymethyl cellulose (CMC) merupakan material kemasan pangan biodegradable yang menjanjikan, tetapi memiliki kekuatan yang rendah dan sensitivitas yang tinggi terhadap air. Penelitian ini mengkaji pengaruh silika (0–0,45 g) pada film WPI/CMC yang mengandung 0,75 atau 1,0 g CMC. Parameter yang dievaluasi meliputi ketebalan, swelling (pengembangan), kuat tarik, perpanjangan putus, biodegradasi melalui penguburan dalam tanah, SEM, dan FTIR. Penambahan silika meningkatkan ketebalan dari 0,126–0,145 mm menjadi 0,350–0,371 mm dan menurunkan swelling dari 83,23% menjadi 63,33% (0,75 g CMC) serta dari 79,23% menjadi 60,86% (1,0 g CMC). Kuat tarik mencapai puncak pada 0,35 g silika, yaitu 27,07 MPa (0,75 g CMC), atau 13,4 kali lipat dari kontrol, kemudian menurun pada 0,45 g, sejalan dengan aglomerasi partikel yang teramati melalui SEM. Perpanjangan putus tertinggi (58,52%) diperoleh pada 1,0 g CMC dengan 0,05 g silika. Biodegradasi menurun seiring peningkatan kadar silika, dari sekitar 83% menjadi 60% (0,75 g CMC) dan dari sekitar 75% menjadi 59% (1,0 g CMC), dengan hampir semua film memenuhi ambang batas SNI 7188.7:2016 sebesar 60%. Hasil FTIR tidak menunjukkan pita serapan baru, kecuali Si–O–Si, yang mengindikasikan adanya interaksi fisik tanpa modifikasi kimia pada polimer. Dengan demikian, film WPI/CMC berpengisi silika berpotensi sebagai kemasan biodegradable yang tahan air, dengan kisaran silika yang bermanfaat sebesar 0,05–0,35 g.
Kata Kunci: *whey protein isolate; carboxymethyl cellulose; silika; film biokomposit; biodegradabilitas; kemasan pangan*

1. Introduction

Food packaging is indispensable for preserving the quality and safety of food products, as it protects them from oxygen, moisture, light, and microbial contamination throughout storage, transportation, and distribution [1]. By slowing physicochemical deterioration and microbial spoilage, effective packaging extends shelf life and reduces food loss and waste, which remain critical challenges for global food security [2]. Yet this function has long relied on petroleum-based polymers that are non-biodegradable, persist in the environment for decades, and contribute to plastic pollution and greenhouse gas emissions [1].

Consequently, biodegradable packaging materials have gained considerable attention as a strategy that simultaneously maintains food quality, prolongs shelf life, and supports environmental conservation [2], [3]. In this regard, bio-based polymers, namely polysaccharides, lipids, and proteins, represent a viable alternative to petroleum-derived polymers, as they utilize abundant renewable resources while addressing the growing demand for sustainable materials [3; 4].

Among protein-based biopolymers, whey protein isolate (WPI) has attracted particular interest as a film-forming material. WPI is a high-protein biological derivative recovered from whey, a by-product of cheese production, so its use also adds value to dairy-industry waste streams [5; 6]. WPI films exhibit excellent film-forming ability and outstanding gas-barrier properties, notably against oxygen, which in several reports exceed those of petroleum-based polymers [7]. Nevertheless, their practical application is constrained by poor moisture resistance and weak mechanical properties, both of which stem from the abundance of hydrophilic amino acid residues in the protein structure [8]. To overcome these drawbacks, WPI has been modified with nano-sized carboxymethyl cellulose (CMC) [9; 12].

CMC is a cellulose derivative obtained through etherification of native cellulose. It is inexpensive and readily available, and it is widely used as a stabilizer and thickener in food systems as well as a matrix component and plasticizer in bioplastics and biocomposite films, often through crosslinking strategies. Beyond its technological functionality, CMC influences the end-of-life behavior of bioplastics: higher CMC content has been reported to accelerate microbial biodegradation significantly. CMC also yields a smoother film surface, indicating improved compatibility and homogeneity within the polymer matrix. Nevertheless, the dissolution of biocomposite films in water remains a challenge, since biopolymer molecules entrap water within the network, as reported for starch-based systems, and thereby reduce film solubility. To further improve film characteristics, environmentally benign fillers such as silica have been introduced into biocomposite formulations [13;15].

Silica is widely employed as a filler owing to its porous structure, high surface activity, and good biocompatibility, which promote interfacial interactions with the polymer matrix [13], [16; 18]. Increasing silica concentration is expected to directly alter the physical and mechanical characteristics of the resulting films. However, the effect of silica on WPI/CMC biocomposite systems has not been systematically investigated. Therefore, this study aimed to evaluate the thickness, water absorption, structural and morphological properties, mechanical properties, and biodegradability under environmental conditions of silica-reinforced WPI/CMC biocomposite films. The structural and morphological properties were characterized by Fourier transform infrared (FTIR) spectroscopy and scanning electron microscopy (SEM), whereas the mechanical properties were assessed through tensile strength and elongation at break.

2. Material and Methods

2.1 Materials

Whey protein isolate (WPI, protein content ≥90%) was purchased from Sigma-Aldrich (USA). Sodium carboxymethyl cellulose (CMC, degree of substitution 0.7, medium viscosity) and silica (SiO_2, particle size ~20 nm, purity ≥99%) were obtained from Merck (Germany). Distilled water was used as the solvent throughout the study. All reagents were used as received without further purification.

2.2 Preparation of WPI/CMC solution

WPI (5 g) was dissolved in 100 mL of distilled water using a magnetic stirrer at 400 rpm and room temperature (25 ± 2 °C) for 1.5 h. The solution was then heated at 70 °C for 1 h under continuous stirring. CMC was subsequently added at two loadings (0.75 and 1.0 g) to the warm WPI solution and stirred at 400 rpm for 30 min prior to cooling.

2.3 Preparation of silica dispersion

Silica (0.05, 0.15, 0.25, 0.35, and 0.45 g) was dispersed in 50 mL of distilled water using an ultrasonic bath (40 kHz, 100 W) for 1 h at room temperature. The dispersion was then heated at 70 °C for 30 min under stirring.

2.4 Fabrication of biocomposite films

The WPI/CMC solution and the silica dispersion were mixed under magnetic stirring at 400 rpm for 30 min at 70 °C. The resulting mixture was cast into polystyrene Petri dishes (diameter 9 cm, 25 mL per dish) and dried at 55 °C for 24 h in an oven. The dried films were cooled to room temperature and peeled off, then conditioned at 25 °C and 50 ± 5% relative humidity for 48 h before characterization. Film codes are summarized in Table 1.

Table 1. Film codes and compositions.

Code	WPI (g)	CMC (g)	Silica (g)
W/C0.75-S0.05	5	0.75	0.05
W/C0.75-S0.15	5	0.75	0.15
W/C0.75-S0.25	5	0.75	0.25
W/C0.75-S0.35	5	0.75	0.35
W/C0.75-S0.45	5	0.75	0.45
W/C1.0-S0.05	5	1.00	0.05
W/C1.0-S0.15	5	1.00	0.15
W/C1.0-S0.25	5	1.00	0.25

2.5 Characterization of biocomposite films

2.5.1 Thickness

Films were cut into 2 × 2 cm specimens, and thickness was measured with a digital caliper (accuracy 0.01 mm) at five random positions per specimen. The mean value was reported [14].

2.5.2 Swelling

Film specimens (50 mm in length) were weighed (W_0), immersed in 50 mL of distilled water at 25 °C for 24 h, blotted with tissue paper to remove surface water, and reweighed (W_t). Swelling was calculated as:

Swelling (%) = $[(W_t - W_0) / W_0] \times 100$

2.5.3 Tensile strength and elongation at break

Tensile strength (TS) and elongation at break (EB) were determined according to ASTM D882 using a Computer Universal Testing Machine HT-2402 equipped with a 100 N load cell. Specimens (10 × 1 cm) were clamped with an initial grip separation of 50 mm and stretched at a crosshead speed of 10 mm/min. TS was obtained from the maximum load recorded automatically by the instrument divided by the initial cross-sectional area, and EB was calculated as the percentage change in length at fracture relative to the initial length [18]. Each measurement was performed in triplicate.

2.5.4 Biodegradability (soil burial test)

Specimens (2 × 2 cm) were weighed (W_0) and buried at a depth of 5 cm in garden soil (moisture maintained at ~40%, ambient temperature 28 ± 2 °C). At predetermined intervals (3, 6, 9, and 12 days), the samples were retrieved, gently cleaned of soil, dried at 50 °C to constant weight, and reweighed (W_t). Weight loss was calculated as:

Weight loss (%) = $[(W_0 - W_t) / W_0] \times 100$ [19], [20]

2.5.5 Morphology (SEM)

The surface and cross-sectional morphology of the 2 × 2 cm specimens was examined by scanning electron microscopy (SEM, JEOL JSM-6510LA) at an accelerating voltage of 10 kV and magnifications of 500× and 2000×. Samples were sputter-coated with gold prior to observation. The micrographs were also used to evaluate the distribution of silica filler within the polymer matrix.

2.5.6 Functional group analysis (FTIR)

FTIR spectra were recorded on a Shimadzu IR Prestige-21 spectrophotometer in ATR mode over the range of 4000–500 cm^{-1} at a resolution of 4 cm^{-1} with 32 scans [15].

2.5.7 Statistical analysis

Data are presented as mean ± standard deviation (n = 3). Differences among samples were analyzed by one-way ANOVA followed by Tukey's post hoc test at $p < 0.05$ using SPSS software.

3. Results and Discussion

3.1 Film thickness

The thickness of the WPI/CMC biocomposite films containing 0.75 and 1.0 g of CMC with silica loadings of 0, 0.05, 0.15, 0.25, 0.35, and 0.45 g is shown in Fig. 1. Film thickness ranged from 0.126 to 0.371 mm. The control films (without silica) were the thinnest, at approximately 0.126 mm (0.75 g CMC) and 0.145 mm (1.0 g CMC). Thickness increased steadily with silica content in both series, reaching approximately 0.350 mm for 0.75 g CMC and 0.371 mm for 1.0 g CMC at 0.45 g silica, i.e., roughly 2.6- to 2.8-fold higher than the respective controls.

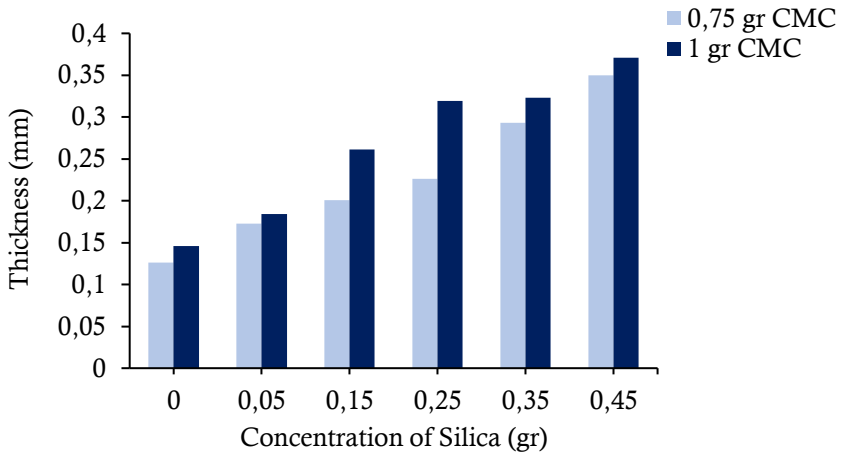

Fig. 1. Effect of silica content on the thickness of WPI/CMC biocomposite films (mean ± SD, n = 5).

Fig. 1. Effect of silica content on the thickness of WPI/CMC biocomposite films (mean ± SD, n = 5). At every silica loading, films containing 1.0 g of CMC were thicker than those containing 0.75 g. The difference was small at low silica content (≈0.01 mm at 0.05 g) but widened at intermediate loadings, reaching ≈0.09 mm at 0.25 g silica, and narrowed again at 0.35 and 0.45 g. Because all films were cast from the same solution volume, a higher CMC or silica content increases the total solid mass per unit casting area, which results in thicker films. In addition, the silica particles act as fillers that occupy space within the polymer network and increase the film volume.

For food packaging, the maximum thickness of 0.25 mm specified by the Japanese Industrial Standard (JIS) [ref. to be added] was used as the reference. For the 0.75 g CMC series, films containing up to 0.25 g silica (≈0.225 mm) met this limit, whereas those with 0.35 and 0.45 g exceeded it. For the 1.0 g CMC series, only films with up to 0.05 g silica were clearly below the limit, while films with 0.15 g silica (≈0.26 mm) were at the limit and those with 0.25 g and above exceeded it.

3.2 Swelling of biocomposite films

The swelling degree of the films was determined from the mass gain after water immersion and reflects the amount of water absorbed by the film matrix. The results for films with 0.75 and 1.0 g CMC and silica loadings of 0 to 0.45 g are shown in Fig. 2. Swelling decreased progressively with increasing silica content in both CMC series. For the 0.75 g CMC series, swelling fell from 83.23% (control) to 79.61%, 75.48%, 73.29%, 68.56%, and 63.33% at 0.05, 0.15, 0.25, 0.35, and 0.45 g silica, respectively. For the 1.0 g CMC series, swelling fell from 79.23% (control) to 73.84%, 71.21%, 68.95%, 66.72%, and 60.86%. At the highest silica loading (0.45 g), swelling was thus reduced by about 24% (0.75 g CMC) and 23% (1.0 g CMC) relative to the respective controls.

At every silica loading, films with 1.0 g CMC swelled less than those with 0.75 g CMC. The difference was largest at 0.05 g silica (5.77 percentage points) and smallest at 0.35 g (1.84 percentage points). Because CMC is hydrophilic, this result is not intuitive. It may be explained by stronger hydrogen bonding and electrostatic interaction between CMC and WPI, which produce a denser, more tightly bound network that restricts chain mobility and water penetration. Thicker films (Section 3.1) also have a lower

surface-area-to-volume ratio, which may reduce the apparent swelling. These explanations are proposed here as hypotheses and are not directly tested.

The reduction in swelling with silica is attributed to the filler effect. Silica particles are dispersed within the WPI/CMC matrix, where they can form hydrogen bonds with polar groups (–OH, –NH_2, –COOH) of the polymers. This interaction reduces the number of hydrophilic sites available to water, increases matrix density and rigidity, and limits the free volume and chain relaxation required for water uptake. Lower swelling is desirable for food packaging because it indicates better water resistance and dimensional stability. Films with lower swelling are less likely to soften, deform, or lose mechanical integrity in humid conditions.

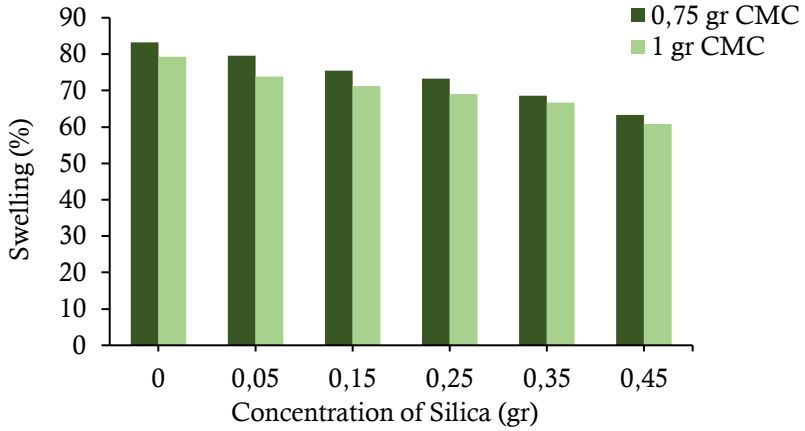

Fig. 2. Effect of silica content on the swelling of WPI/CMC biocomposite films (mean ± SD, n = 3).

3.3 Tensile strength and elongation at break

The mechanical properties of the biocomposite films are summarized in Table 2. Tensile strength (TS) of the control films was low, at 2.02 MPa (0.75 g CMC) and 2.65 MPa (1.0 g CMC). Adding silica increased TS in both series up to 0.35 g, followed by a decline at 0.45 g. In the 0.75 g CMC series, TS rose from 2.02 to 4.02, 4.90, 10.00, and 27.07 MPa at 0.05 to 0.35 g silica, a 13.4-fold increase over the control, and then fell to 16.28 MPa at 0.45 g. In the 1.0 g CMC series, TS rose from 2.65 to 8.34, 12.06, 12.45, and 14.91 MPa (5.6-fold) and then fell to 9.41 MPa at 0.45 g. Even at the highest silica loading, TS remained above the respective control (about 8.1-fold and 3.6-fold).

Table 2. Tensile strength and elongation at break of WPI/CMC/silica biocomposite films

CMC (g)	Silica (g)	Tensile strength (MPa)	Elongation at break (%)
0.75	0	2.02	7.42
	0.05	4.02	26.48
	0.15	4.90	26.08
	0.25	10.00	13.60
	0.35	27.07	14.36
	0.45	16.28	8.32
1.00	0	2.65	9.92
	0.05	8.34	58.52
	0.15	12.06	28.48

CMC (g)	Silica (g)	Tensile strength (MPa)	Elongation at break (%)
	0.25	12.45	18.24
	0.35	14.91	18.20
	0.45	9.41	16.00

The improvement in TS is attributed to the reinforcing effect of silica. Its surface silanol (Si–OH) groups can form hydrogen bonds with the hydroxyl, carboxyl, and amino groups of WPI and CMC, strengthening filler–matrix interaction and allowing stress to be transferred from the matrix to the particles. Hydrogen bonds of this kind are difficult to break and require considerable energy. The decrease at 0.45 g silica is likely caused by particle agglomeration. Silica is insoluble in water and can only be dispersed, so at high loading the particles tend to cluster, become unevenly distributed, and reduce the effective filler–matrix contact area. The clusters then act as stress concentration points that initiate failure at lower loads. This explanation should be confirmed with the SEM micrographs (Section 3.x).

Elongation at break (EB) ranged from 7.42 to 58.52% (**Table 2**) and followed a different trend. EB first rose sharply with the smallest silica addition (0.05 g), from 7.42% to 26.48% (0.75 g CMC) and from 9.92% to 58.52% (1.0 g CMC), which was the highest value in the study. This indicates that a small amount of well-dispersed silica did not embrittle the films and improved their strength and extensibility together. Beyond 0.05 g, EB decreased with increasing silica content. In the 1.0 g CMC series it fell steadily from 58.52% to 28.48, 18.24, 18.20, and 16.00%. In the 0.75 g CMC series it fell from 26.48% to 26.08, 13.60, 14.36, and 8.32%, with a slight increase at 0.35 g. The decrease in EB at higher loadings reflects the restriction of polymer chain mobility by the rigid filler and the stiffer, more compact network, which makes the films less deformable. This gives the commonly reported inverse relationship between TS and EB, which is seen here at silica contents above 0.05 g. At 0.05 g, both TS and EB increased together.

The effect of CMC content is also visible in the data. The 1.0 g CMC films had higher EB than the 0.75 g films at all silica loadings. They also had higher TS at silica loadings up to 0.25 g, but lower TS at 0.35 g (14.91 vs. 27.07 MPa) and 0.45 g (9.41 vs. 16.28 MPa). This suggests that the higher CMC content increases the viscosity of the film-forming solution and may promote earlier silica agglomeration, although this was not directly tested.

3.4 Biodegradability of biocomposite films

Biodegradability was evaluated by the soil burial test to assess how readily the films are broken down by soil microorganisms. The degree of biodegradation was calculated as the weight loss relative to the initial dry weight, i.e., $[(W_0 - W_t)/W_0] \times 100$, where W_0 is the dry weight before burial and W_t is the dry weight after burial. The results for films with 0.75 and 1.0 g CMC and silica loadings of 0 to 0.45 g are presented in Fig. 3. Biodegradation decreased progressively as silica content increased in both CMC series. For the 0.75 g CMC series, it fell from approximately 83% (control) to about 75, 70, 69, 65, and 60% at 0.05, 0.15, 0.25, 0.35, and 0.45 g silica, respectively. For the 1.0 g CMC series, it fell from approximately 75% (control) to about 70, 68, 63, 61, and 59%. The highest value in the study was recorded for the control film with 0.75 g CMC (≈83%), and the highest value among silica-filled films was for 0.75 g CMC with 0.05 g silica (≈75%). The lowest value was found for the film with 1.0 g CMC and 0.45 g silica (≈59%).

At every silica loading, films with 1.0 g CMC degraded less than those with 0.75 g CMC, although the gap narrowed at high silica content (≈1 percentage point at 0.45 g). Soil microbial attack on protein/polysaccharide films depends on water uptake, because water swells the matrix and allows microbial enzymes to reach the polymer chains. The lower biodegradation at higher CMC content is therefore consistent with the lower swelling of the 1.0 g CMC films (Section 3.2) and with the denser WPI–CMC network. The decrease with silica is also consistent with the swelling results. Silica reduces water uptake and increases matrix density, and its inorganic, poorly degradable particles reduce the fraction of the film that is biodegradable. Together these effects limit water penetration and microbial access, so the films degrade more slowly. Water absorption and biodegradation therefore follow the same trend, and both decrease with silica loading.

According to SNI 7188.7:2016, a bioplastic should reach a degradation of more than 60%. Based on **Fig. 3**, nearly all films met this requirement. The film with 0.75 g CMC and 0.45 g silica (≈60%) was at

the threshold, while the 1.0 g CMC films with 0.35 and 0.45 g silica were close to it (≈61 and ≈59%). Because the burial time was 14 days, these values should be interpreted as degradation after that period only.

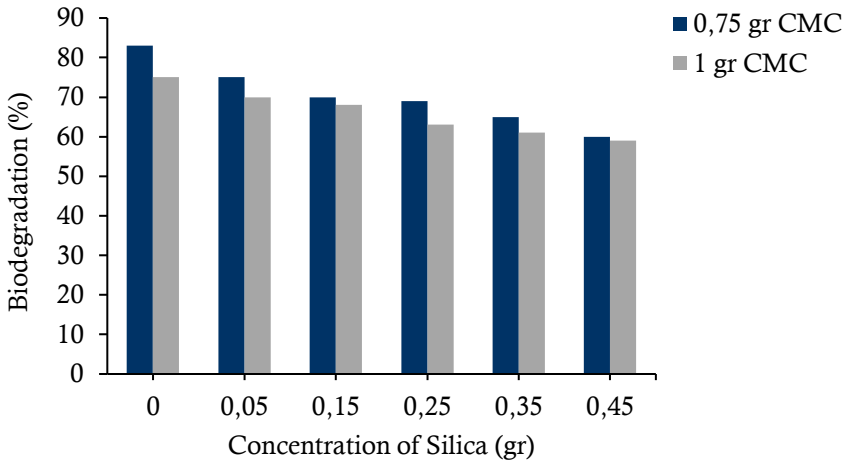

Fig. 3. Effect of silica content on the biodegradation of WPI/CMC biocomposite films after 14 days of soil burial (mean ± SD, n = 3).

3.5 Surface morphology of biocomposite films (SEM)

The surface morphology of the WPI/CMC films containing 0, 0.05, 0.15, 0.25, 0.35, and 0.45 g of silica is shown in **Fig. 4**, with panel (a) for the 0.75 g CMC series and panel (b) for the 1.0 g CMC series. The micrographs show that silica content changed the surface structure of the films. The control films (without silica) of both series, Fig. 4(a-a) and 4(b-a), had uneven surfaces with visible voids. Films containing silica (Fig. 4a-b to 4a-f and 4b-b to 4b-f) were also rough, but the surface looked more compact and had fewer voids than the controls. Small bright particles, marked with circles and arrows in the micrographs, were observed on the surfaces of several silica-filled films, and they are attributed to silica particles embedded in or deposited on the WPI/CMC matrix. These particles appear as small, scattered features at low silica content [state which panels]. At higher loadings, especially in the 1.0 g CMC series at 0.45 g silica (Fig. 4b-f), larger clustered features were observed, which indicate particle agglomeration.

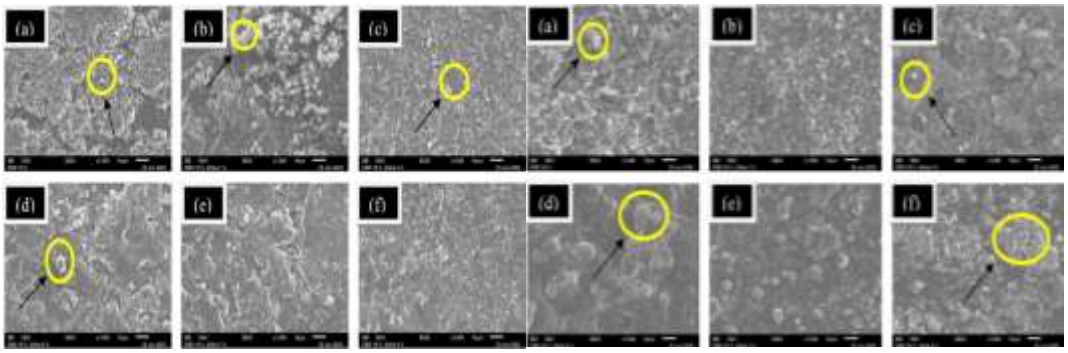

(a) (b)

Fig. 4. SEM micrographs of the surface of WPI/CMC biocomposite films: (a) 0.75 g CMC and (b) 1.0 g CMC, with silica contents of (a) 0, (b) 0.05, (c) 0.15, (d) 0.25, (e) 0.35, and (f) 0.45 g. Circles and arrows indicate silica particles/agglomerates.

The fewer voids in the silica-filled films are consistent with the filler effect. Silica particles occupy the free space within the polymer network and interact with the polar groups of WPI and CMC, which produces a denser matrix. This agrees with the lower swelling (Section 3.2), the higher tensile strength at low to intermediate silica loading (Section 3.3), and the lower biodegradation (Section 3.4). The uneven surface is attributed to non-uniform particle distribution during film formation and to particle aggregation, since silica is only dispersed, not dissolved, in the aqueous film-forming solution. The agglomerates seen

at high loading support the decline in tensile strength and elongation at 0.45 g silica reported in Section 3.3, because clusters act as stress concentration points.

3.6 Functional groups of biocomposite films (FTIR)

FTIR spectroscopy was used to identify the functional groups of the films and the interactions among WPI, CMC, and silica. The spectra of the films with 0.75 g CMC (Fig. 5a) and 1.0 g CMC (Fig. 5b) at different silica loadings are shown in Fig. 5. All spectra show the same set of bands, and silica addition did not produce new bands other than those of Si-O-Si. A broad O-H stretching band appears in the high-wavenumber region [≈3600-3000 cm^{-1}]. It is assigned to the hydroxyl groups of CMC and silica (Si-OH), the N-H/O-H groups of WPI, and adsorbed water, and its breadth indicates extensive hydrogen bonding within the film. Bands attributed to C=O stretching [≈1800-1600 cm^{-1} range] originate from the carboxyl/carboxylate groups of CMC and the amide groups of WPI. A band in the 1103-803 cm^{-1} region is assigned to the asymmetric and symmetric stretching of Si-O-Si, which confirms the presence of silica in the films. This band is weak in the spectra, so its intensity/position change with silica content should be stated after checking the data. The same bands appear in all twelve samples, so the polymer backbones were not chemically altered.

The relative intensity of the O-H band varied among samples (Fig. 5), but not in a systematic order with silica content. Any shift or broadening of the O-H and C=O bands relative to the control would indicate hydrogen bonding between the Si-OH groups of silica and the polar groups of WPI and CMC. This is consistent with the lower swelling (Section 3.2) and higher tensile strength (Section 3.3) of the silica-filled films. The presence of hydrophilic groups (O-H, C=O) in the matrix also allows water uptake, which can promote microbial attack during soil burial.

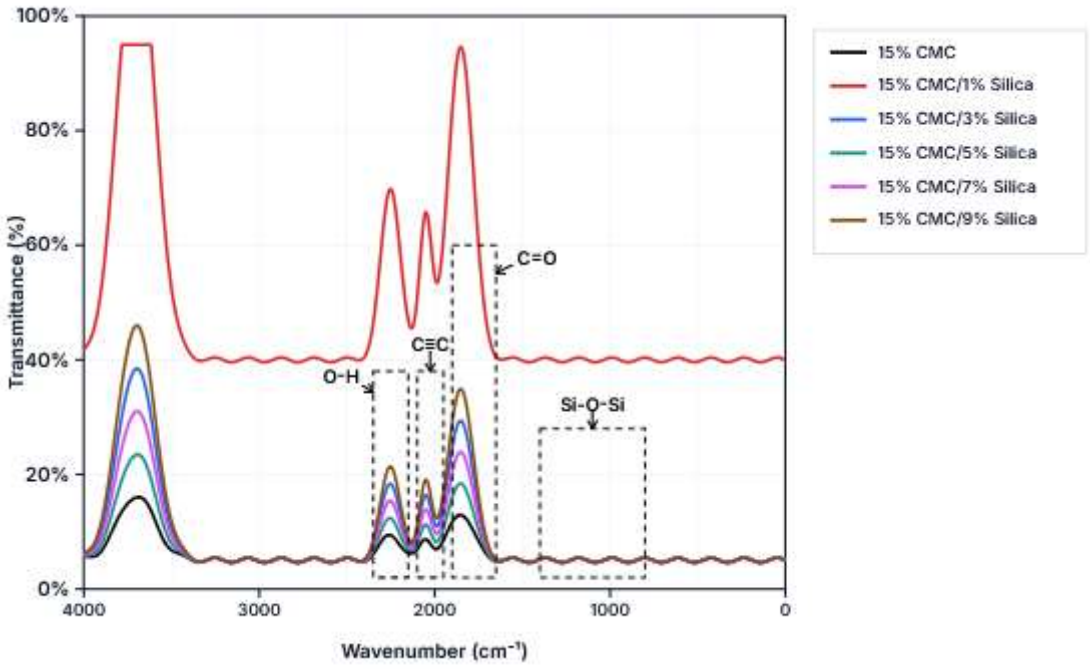

(a)

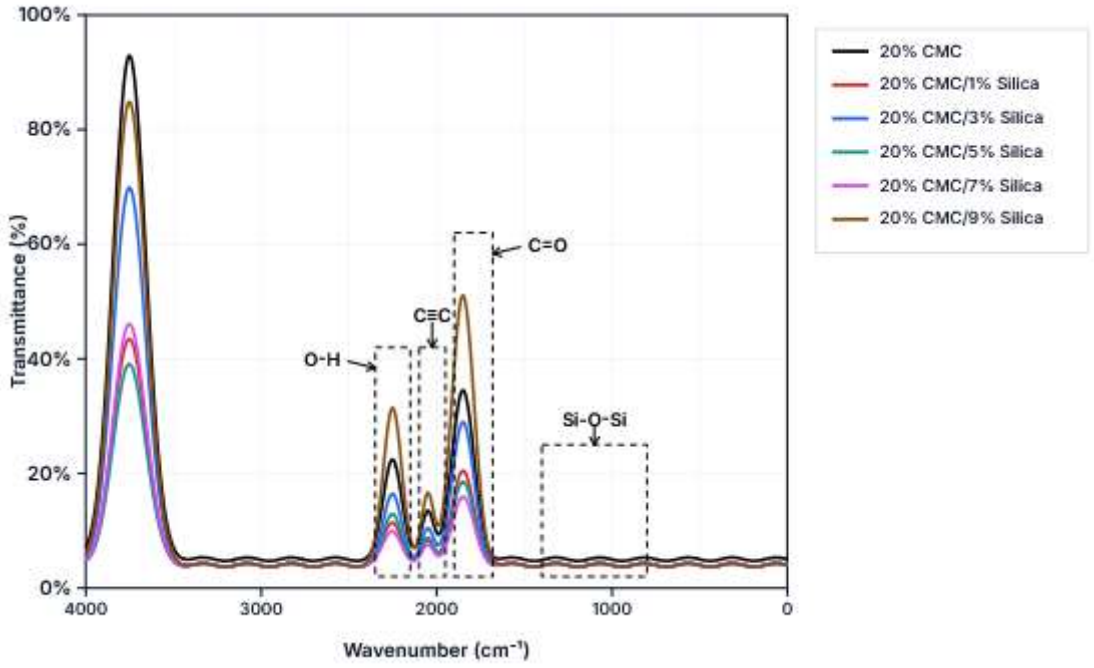

(b)

Fig. 5. FTIR spectra of WPI/CMC biocomposite films with different silica contents: (a) 0.75 g CMC and (b) 1.0 g CMC.

4. Conclusion

Silica content strongly influenced the properties of WPI/CMC biocomposite films. Increasing silica raised film thickness and lowered swelling and biodegradation, while tensile strength improved up to 0.35 g silica (27.07 MPa at 0.75 g CMC) before declining at 0.45 g because of agglomeration. The highest elongation at break (58.52%) was obtained with 1.0 g CMC and 0.05 g silica, where strength and extensibility increased together. Only 0.75 g CMC films with up to 0.25 g silica met the 0.25 mm thickness limit, and nearly all films met the 60% biodegradation requirement. FTIR showed no chemical alteration of the polymers. Overall, 0.75 g CMC with 0.25 g silica appears to give a balanced combination of thickness, strength, and degradability.

5. Acknowledgment

The authors gratefully acknowledge colleagues at Universitas Syiah Kuala for their valuable technical support and scientific discussions that contributed to this research. The interpretations and conclusions presented in this paper are solely those of the authors.

6. References

[1] Y. Yin and M. W. Woo, “Transitioning of petroleum-based plastic food packaging to sustainable bio-based alternatives,” Sustain. Food Technol., vol. 2, no. 3, pp. 548–566, 2024.
[2] J. R. Westlake, M. W. Tran, Y. Jiang, X. Zhang, A. D. Burrows, and M. Xie, “Biodegradable biopolymers for active packaging: Demand, development and directions,” Sustain. Food Technol., vol. 1, no. 1, pp. 50–72, 2023.
[3] S. M. El-Sayed and A. M. Youssef, “Eco-friendly biodegradable nanocomposite materials and their recent use in food packaging applications: A review,” Sustain. Food Technol., vol. 1, pp. 215–227, 2023.
[4] J. Sarfraz, T. Gulin-Sarfraz, J. Nilsen-Nygaard, and M. K. Pettersen, “Nanocomposites for food packaging applications: An overview,” Nanomaterials, vol. 11, no. 1, p. 10, 2021.
[5] M. Danish, “Advances in protein-based biodegradable films: A review,” J. Packag. Technol. Res., vol. 8, no. 2, pp. 109–119, 2024.
[6] A. F. Pires, O. Díaz, A. Cobos, and C. D. Pereira, “A review of recent developments in edible films and coatings: Focus on whey-based materials,” Foods, vol. 13, no. 16, p. 2638, 2024.

[7] V. Chaudhary, P. Kajla, P. Kumari, S. P. Bangar, A. Rusu, M. Trif, and J. M. Lorenzo, "Milk protein-based active edible packaging for food applications: An eco-friendly approach," Front. Nutr., vol. 9, p. 942524, 2022.
[8] A. Etxabide, M. Arregi, S. Cabezudo, P. Guerrero, and K. de la Caba, "Whey protein films for sustainable food packaging: Effect of incorporated ascorbic acid and environmental assessment," Polymers, vol. 15, no. 2, p. 387, 2023.
[9] K. F. Silva, C. S. Marques, A. de Freitas Junior, M. V. Dias, and F. A. Mori, "Whey protein isolate and kraft lignin multifunctional films for potential food packaging application: UV block and antioxidant potential," Food Biosci., vol. 53, p. 102581, 2023.
[10] D. B. Resende et al., "Characterization of antimicrobial and antioxidant performance of dihydroeugenol and its glycoside incorporated into whey protein isolate films," Front. Food Sci. Technol., vol. 3, p. 1237638, 2023.
[11] Y. Wang, J. Wang, J. Lai, X. Zhang, Y. Wang, and Y. Zhu, "Preparation and characterization of chitosan/whey isolate protein active film containing TiO2 and white pepper essential oil," Front. Nutr., vol. 9, p. 1047988, 2022.
[12] Q. Xin et al., "Multifunctional whey protein composite films: Material design and AI integration for next-generation food packaging," Trends Food Sci. Technol., vol. 168, p. 105502, 2026.
[13] W. Zhang, H. Ahari, Z. Zhang, and S. M. Jafari, "Role of silica (SiO2) nano/micro-particles in the functionality of degradable packaging films/coatings and their application in food preservation," Trends Food Sci. Technol., vol. 133, pp. 75–86, 2023.
[14] M. Riza, I. Zuwanna, N. Nuraini, A. E. Mawarni, S. D. Said, M. Mukhlishien, and R. Dewi, "Biocomposite film properties of whey protein isolate/PVA-silica," Results Eng., vol. 26, p. 104514, 2025.
[15] I. Zuwanna, M. Riza, S. Aprilia, Y. Syamsuddin, S. Said, and R. Dewi, "Investigation of characteristics of whey protein isolate/chitosan with silica addition in biocomposite film," Int. J. Technol., vol. 16, no. 1, pp. 359–369, 2025.
[16] S. Sagar, U. Khalid, W. Azim, M. Kanwal, and N. Hossain, "Reinforcement of biodegradable SiO2NPs-modified cellulose-gelatin hydrogel films with antioxidant and antibacterial properties as potential food packaging composite," J. Cluster Sci., vol. 35, pp. 1613–1624, 2024.
[17] C. O. Marinho, L. Marangoni Júnior, R. R. R. Cecci, and R. P. Vieira, "Blends of chitosan and water kefir grain biomass incorporated with nanosilica," Coatings, vol. 13, no. 2, p. 465, 2023.
[18] G. Liu, K. Shi, H. Sun, B. Yang, and Y. Weng, "Nano-SiO_2-modified xylan-PVOH-based composite films: Mechanical and barrier properties investigation," BioResources, vol. 18, no. 2, pp. 4195–4211, 2023.
[19] S. S. Rumi, S. Liyanage, and N. Abidi, "Soil burial-induced degradation of cellulose films in a moisture-controlled environment," Sci. Rep., vol. 14, p. 6921, 2024.
[20] Z. Abbasi, H. Motamedi, Z. Zirrahi, M. Taghavi, A. Farrokhnia, E. Aghaie, and Y. Behnamian, "Nanocomposites for packaging applications: Synthesis, characterization, thermal and microbial degradation of its residues for plant growth," Pollution, vol. 8, no. 1, pp. 133–145, 2022.